VII

Publication VII

J. Häkli, T. Koskinen, J. Ala-Laurinaho, and A. V. Räisänen, "Dual reflector feed system for hologram-based compact antenna test range," *IEEE Transactions on Antennas and Propagation*, vol. 53, no. 12, pp. 3940–3948, Dec. 2005.

Dual Reflector Feed System for Hologram-Based Compact Antenna Test Range

Janne Häkli, *Member, IEEE*, Tomi Koskinen, *Student Member, IEEE*, Juha Ala-Laurinaho, and Antti V. Räisänen, *Fellow, IEEE*

***Abstract*—Manufacturing of large computer-generated submillimeter wave holograms with high pattern accuracy has been the main challenge in the development of hologram based compact antenna test ranges (CATRs). Illumination of the hologram with a shaped beam produced by a dual reflector feed system (DRFS) simplifies the hologram manufacturing by eliminating the narrow slots in the hologram pattern. In this paper, the design of a shaped dual reflector feed for a hologram CATR is described. The simulated and measured illumination field amplitude and phase at 310 GHz are presented and compared to the desired hologram illumination. The measured amplitude is within ± 0.5 dB from the design objective in the most significant central region of the illuminating beam. Measurement results of the quiet-zone field of a demonstration CATR illuminated by the DRFS are presented and compared to the measured quiet-zone amplitude and phase of a hologram fed directly with a corrugated horn. The quiet-zone diameters of the both holograms are over 0.25 meters and the measured root mean squared (rms) amplitude and phase ripples are below ± 0.4 dB and $\pm 5^{\circ}$, respectively. Further improvements to the hologram CATR, such as greater tolerance to manufacturing errors, are also discussed.**

***Index Terms*—Compact range, computer-generated hologram, multireflector antennas, submillimeter wave antennas.**

I. Introduction

THE electrical testing of large millimeter and submillimeter wave reflector antennas is challenging. Hologram based compact antenna test range (CATR) is a good alternative to the conventional CATRs [1]. The hologram pattern is in principle a record of the binarized interference pattern of the incident wave and the desired output wave. When the hologram pattern is illuminated with a spherical wave, the plane wave is generated into the quiet-zone. The pattern is generated iteratively with a computer using finite-difference time-domain (FDTD) method based analysis software [2]. Holograms are inexpensive to manufacture as the planar hologram pattern can be etched on a metal plated dielectric film using photolithography. The film is tensioned into a frame to ensure surface flatness. A schematic of the hologram CATR and an example of the hologram pattern are shown in Fig. 1. The plane wave propagates to the angle of 33° in relation to the hologram normal in order to separate the desired plane wave from other diffraction modes generated by the hologram.

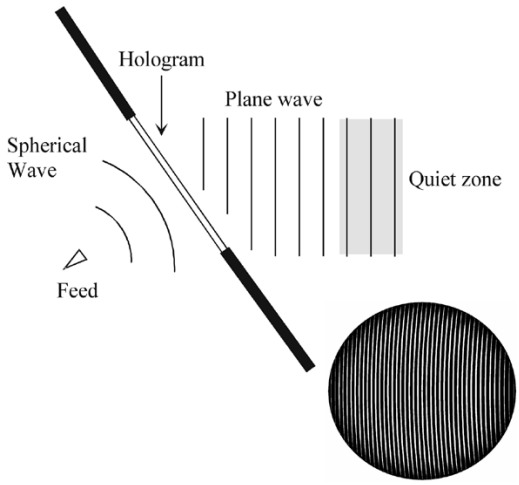

Fig. 1. Hologram based compact antenna test range and an example of the hologram pattern.

The main challenge in the development of submillimeter wave hologram CATRs has been the accurate manufacturing of large holograms. Holograms up to 5 meters in diameter are needed to test large reflector antennas. The hologram pattern consists of narrow curved slots (shown in white in Fig. 1). The slot width controls mostly the amplitude in the hologram transmission and the location of the slots controls the phase. The slots are tapered toward the hologram edge to realize amplitude taper into the hologram aperture field to reduce edge diffraction when the hologram is illuminated directly with a corrugated horn. Narrow slots with widths below 100 μm are difficult to etch accurately.

The amplitude taper can be realized into the hologram illumination by using a dual reflector feed system (DRFS) to shape the beam radiated by a feed horn [3]–[5]. Amplitude tapered hologram illumination allows nearly equal slot widths in the hologram pattern and narrow slots can be avoided in the pattern. In this paper, the design and realization of a DRFS for submillimeter wave hologram CATRs to facilitate the hologram manufacturing is described. The DRFS consists of two hyperboloid-type shaped reflectors. The DRFS operation was verified by simulating and measuring the beam illuminating the hologram at the frequency of 310 GHz. For the same frequency, a demonstration hologram was designed and tested with the dual reflector feed system. We present the simulation and measurement results of the DRFS beam and compare the measured quiet-zone

Manuscript received May 2, 2005; revised July 1, 2005. This work was supported in part by ESA/ESTEC under Contract 13096/98/NL/SB and in part by the Academy of Finland and Tekes through their Centre-of-Excellence program.

The authors are with the MilliLab, Radio Laboratory, SMARAD, Helsinki University of Technology, Espoo FI-02015 TKK, Finland (e-mail: janne.hakli@tkk.fi).

Digital Object Identifier 10.1109/TAP.2005.859900

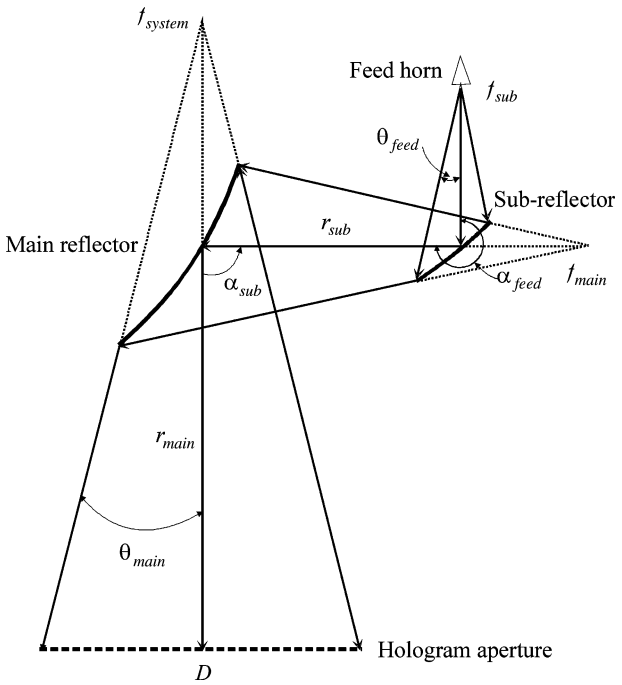

Fig. 2. Dual reflector feed system geometry. The figure is not in scale and the reflectors are enlarged for clarity.

field of the demonstration CATR to a hologram based CATR fed directly with a corrugated horn. We also discuss potential improvements to the hologram based CATRs with a shaped hologram illumination.

II. Design of the DRFS

The design of a dual reflector feed system for hologram based compact antenna test ranges is based on a shaped dual reflector antenna synthesis. A ray tracing based geometrical optics (GO) synthesis procedure was developed for designing the reflector feed system [6], [7]. Geometrical optics based synthesis was selected because GO enables in principle frequency independent design allowing the DRFS to operate over a wide bandwidth. GO employs a high frequency approximation of Maxwell's equations and it is suitable for the analysis of electrically large reflectors. At the submillimeter wavelengths physically relatively small structures can be electrically large, and therefore, GO approach was selected for the DRFS synthesis.

A. Geometry of the System

Dual shaped offset hyperboloid configuration was selected for the feed system as it allows a wide beam with a compact reflector structure. The first reflector is called the subreflector and the larger second reflector is called the main reflector. The geometry of the DRFS is defined by the system focal length $f_{\rm system}$, i.e., the hologram focal length, the diameter of the output aperture D, the distance of the main reflector center from the hologram center $r_{\rm main}$, the focal lengths of the main and subreflectors $f_{\rm main}$ and $f_{\rm sub}$, the distance from the main reflector center to the subreflector center $r_{\rm sub}$, the subreflector offset angle $\alpha_{\rm sub}$, the primary feed offset angle $\alpha_{\rm feed}$, the feed horn half-beam width $\theta_{\rm feed}$, and by the DRFS output half-beam width $\theta_{\rm main}$. The basic system geometry is shown in Fig. 2. The figure is not in scale and the reflectors have been enlarged for clarity. The virtual focus of the main reflector is at the hologram focus and the feed horn phase center is at the focus of the subreflector hyperboloid. The virtual focus of the subreflector coincides with the focus of the main reflector. The final synthesized reflector surfaces are shaped surfaces without clear focal points, but the assumption of nonshaped hyperboloid surfaces is useful for defining the system geometry. The input aperture of the dual reflector feed system is on the subreflector and the output aperture is the hologram aperture. The input and output beam widths ($\theta_{\rm feed}$ and $\theta_{\rm main}$) correspond to the viewing angles of the input and output aperture rim seen from the feed point and from the system focus, respectively.

TABLE I
Selected DRFS Geometry

D=736 mm	α_{sub}=90°
f_{system}=1800 mm	α_{feed}=270°
f_{main}=375 mm	θ_{main}=11.55°
f_{sub}=100 mm	θ_{feed}=21°
r_{main}=1550 mm	
r_{sub}=150 mm	

The geometry of the DRFS is selected so that the direct radiation of the feed horn to the main reflector is avoided and the subreflector blocks the direct radiation from the feed horn to the hologram aperture, i.e., the subreflector spill-over falls outside the hologram and the main reflector. To reduce edge diffraction disturbances in the beam, the edge illumination of below -15 dB was selected for both reflectors. The manufacturing of the DRFS has to be also taken into account in the design and the reflector sizes and the over-all dimensions of system should be minimized. The selected geometrical parameters of the DRFS are shown in Table I.

The selected parameters define a concave hyperboloid subreflector and a convex main reflector. The DRFS was designed for a demonstration hologram with a diameter of 600 mm so that the beam extends outside the hologram rim also, i.e., the output aperture is larger than the hologram. However, due to the geometrical optics based reflector synthesis, the same DRFS can be used also for larger holograms providing that the ratio of the output aperture diameter, i.e., the hologram diameter, to the hologram focal length remains the same, i.e., 1/3.

B. Synthesis of the Reflectors

The reflectors in the DRFS are shaped hyperboloid surfaces and they are determined with shaped dual reflector synthesis. A numerical ray-tracing based geometrical optics (GO) synthesis procedure was developed for designing the DRFS. The synthesis procedure is based on the basic idea described in [8] with approximation of the reflector surfaces with tangential planar sections as in [9]–[11]. The developed synthesis procedure is described in detail in [6].

The developed numerical ray-tracing based reflector synthesis procedure is based on the principles of geometrical optics; on the Snell's reflection law, on the conservation of

energy within flux tubes and the phase is determined by the ray path length. The GO calculations are simplified by making certain approximations: the electromagnetic wave fronts are approximated with local plane waves and the reflector surfaces are assumed locally planar around each ray. The rays contain only phase and amplitude information, i.e., the field is sampled at the ray locations and treated locally as a plane wave. Power is considered to propagate between the rays in flux tubes formed by four adjacent rays.

A simple Butterworth-type amplitude function was selected for the hologram illumination

$$E_{\text{out}}(\rho') = \frac{\beta}{\sqrt{1+\left(\frac{\rho'}{\rho_c}\right)^{2N}}} \tag{1}$$

where ρ' is the radial distance in the polar coordinates in the output aperture. The following values were selected: $\rho_c = 210$ mm and $N = 5$. The output ray distribution of the DRFS is determined with so-called input-output aperture mapping. The output amplitude is scaled by factor β so that the total power in the output aperture is equal to the power in the input aperture. In general, a rotationally symmetric aperture mapping is not possible for offset reflectors [12], but a rotationally symmetric mapping is assumed for simplicity, and the resulting error is neglected.

The ray path length determines the phase in the hologram illumination. The hologram is illuminated by a spherical wave originating from the hologram focus and the rays have path lengths $l(n,m)$ corresponding to this wavefront, i.e., for each ray, the ray path length is given by [6]

$$l(n,m) = \sqrt{\rho'(n,m)^2 + f_{\text{system}}^2} \tag{2}$$

where $\rho'(n,m)$ is the radial distance of the ray (n,m) from the hologram center in the hologram aperture and f_{system} is focal length of the hologram.

The reflector surfaces are synthesized so that the input ray distribution is transformed into the output ray distribution corresponding to the desired hologram illumination determined with the aperture mapping. In the synthesis, the reflector surfaces are assumed locally planar and the surface normal is determined at an anterior point, which is the closest previously computed point in the radial direction on the reflector surfaces. In the ray-tracing synthesis procedure, the first reflector (the subreflector) is assumed to modify the amplitude, i.e., the distribution of the rays, and the second reflector (the main reflector) is used to correct the phase by adjusting the ray path length to correspond to the path length given by (2). The synthesis procedure starts with the center ray, for which the ray path is known from the system geometry and proceeds ray-by-ray toward the reflector rims.

C. Structure of the Designed System

The reflector surfaces are manufactured by milling from metal plates. To form the milling data for the milling process, the synthesized reflector surfaces are post-processed. First, as the reflector rim is numerically specified and the points on the rim are not on a plane, a plane is fitted to the synthesized reflector aperture and this plane is moved outside the reflector rim. The reflector surface is then linearly extrapolated to this plane as the distance to this plane is slightly different for each computed point on the rim. The extrapolated part was selected to be at minimum 50 μm high. Second, the transition from the shaped reflector surface to the surface of the metal plate is rounded by fitting an arc of a circle to the transition at each point in the rim to reduce diffraction. The height of the rounding was selected to be $\lambda/4$ at 310 GHz (about 240 μm) and the radius is selected so that the surface tangent is correct at the end of extrapolated part and on the metal plate surface. The

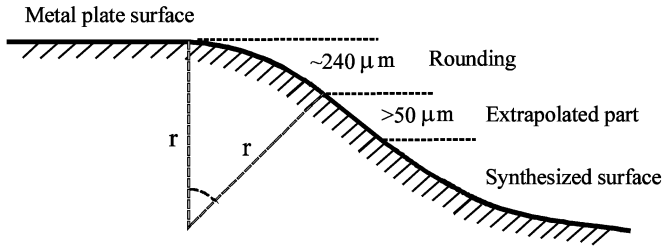

Fig. 3. Reflector edge treatment.

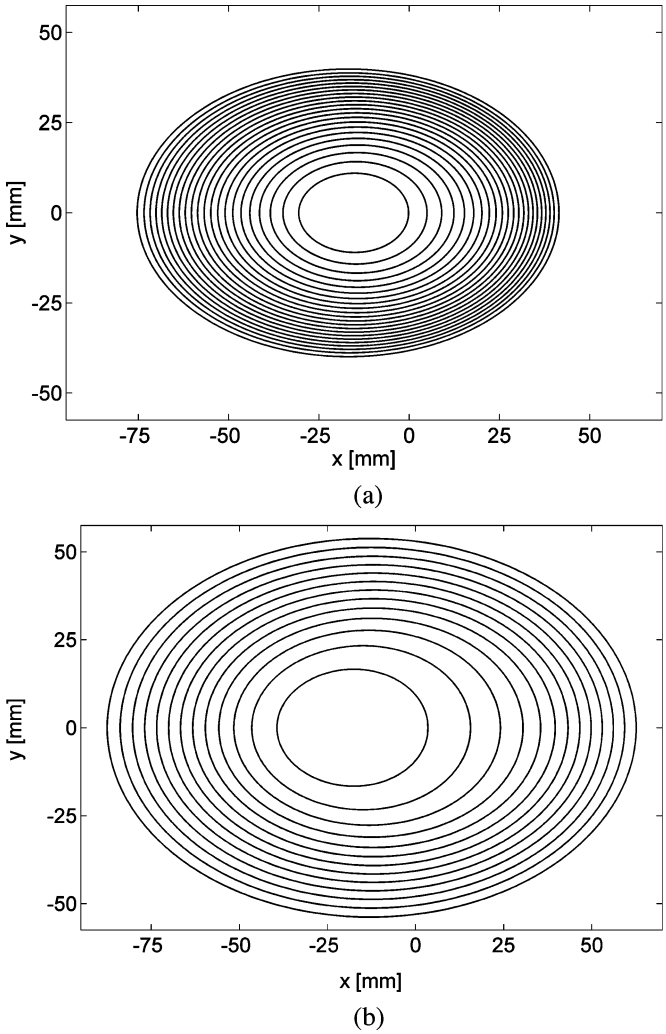

Fig. 4. Contour maps of the synthesized reflector surfaces: (a) concave subreflector and (b) convex main reflector. The contour interval is 200 μm.

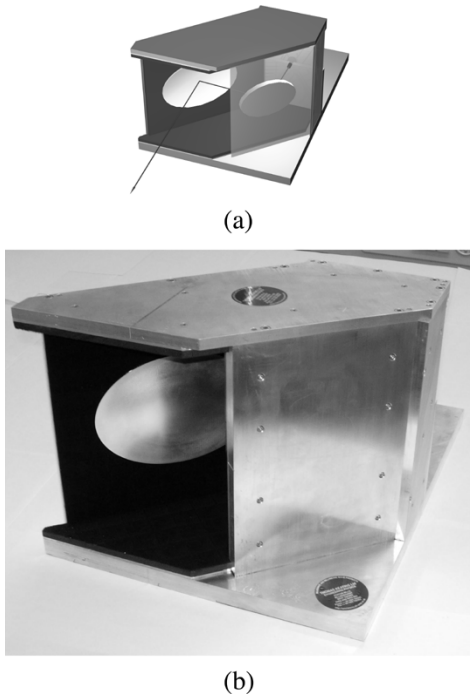

Fig. 5. Dual reflector feed system: (a) a three dimensional model and (b) a photograph of the final DRFS.

reflector edge treatment is illustrated in Fig. 3. The rounding was applied to both reflectors in the DRFS.

The dimensions of the synthesized surfaces including the edge treatment are approximately 122 mm $\times$ 83 mm $\times$ 4.6 mm for the concave subreflector and 165 mm $\times$ 119 mm $\times$ 2.8 mm for the convex main reflector. The synthesized reflector surfaces together with the flat metal plate are shown in Fig. 4. The surfaces are presented in coordinates related to the metal plate on which each reflector is milled. The origin is at the reflection point of the center ray.

The accuracy of the mechanical structure of the dual reflector feed system is critical for the beam quality at submillimeter wavelengths. The surface accuracy of the reflectors should be of the order of $\lambda/100$ or better. The assembly tolerances for the quasioptics are similar. The mechanical structure of the DRFS was designed and manufactured as an integrated quasioptical system at Thomas Keating Engineering Physics, Ltd., in England. An artistic impression of the DRFS and a photograph are shown in Fig. 5. The reflector plates were cut along elliptical rims with the width of 144 and 183 mm and with the height of 88 and 128 mm for the subreflector and for the main reflector, respectively. The elliptical rims were centered to the center reflection points on the reflector surfaces. The reflector plates were attached to the walls of the system and a high precision alignment collar for the feed was constructed to ensure accurate alignment of the quasioptics. The inside of the supporting structure was lined with absorbers (TK THz RAM) to eliminate possible internal reflections.

III. Simulated and Measured DRFS Beam

The performance of the DRFS was verified with simulations and measurements of the beam. The radiated beam of the DRFS

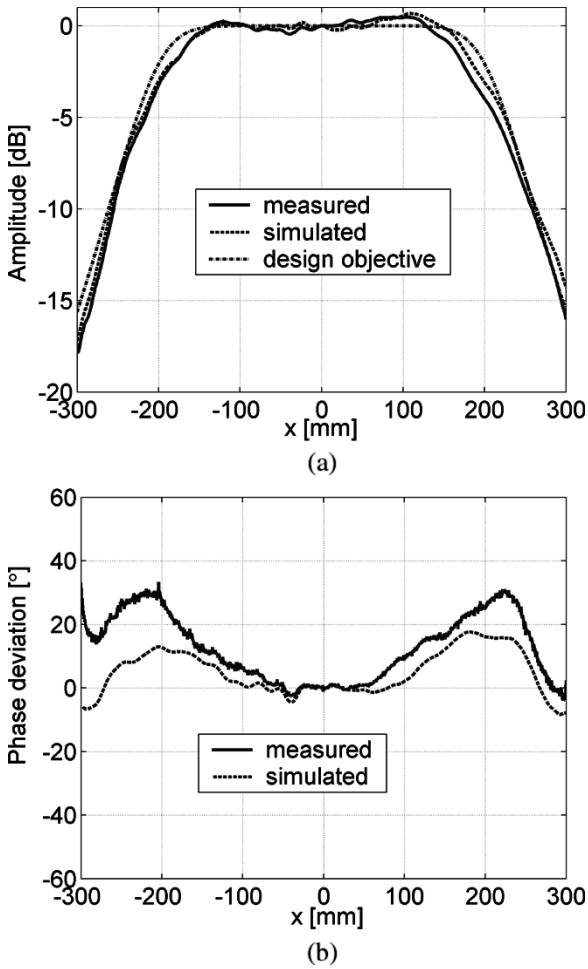

Fig. 6. Measured and simulated (a) amplitude and (b) phase deviation from the spherical wave in a horizontal beam cross-cut at 310 GHz.

was computed with GRASP8W software using physical optics (PO) and physical theory of diffraction (PTD). The simulations (and measurements) were done at 310 GHz, which was selected as the frequency for a demonstration hologram-based CATR. The field illuminating a 600 mm hologram located 1800 mm from the system focus was calculated on the plane of the hologram aperture. The simulation results are shown together with the measured results in Figs. 6 and 7.

The amplitude and phase of the radiated beam of the feed system were measured with a millimeter wave planar scanner at the planned location of the hologram aperture [3], [5]. A millimeter wave vector network analyzer, AB Millimétre MVNA-8-350, with submillimeter wave extensions ESA-1 and ESA-2 as the transmitter and the receiver, was used in the measurements at 310 GHz. The potential error sources affecting the accuracy in planar near-field measurement are listed in [13]. The most significant error sources for the phase in the one-dimensional pattern cuts were identified to be the DRFS misalignment in relation to the scanner, the planarity errors of the scanner (resulting into errors in the probe z-position), the probe xy-positioning errors, and the cable flexing [14]. In two-dimensional contour map measurements, the drift and the temperature stability are significant phase measurement error sources.

The DRFS was aligned perpendicularly to the scanner plane by using a digital feeler pin attached to an extension arm

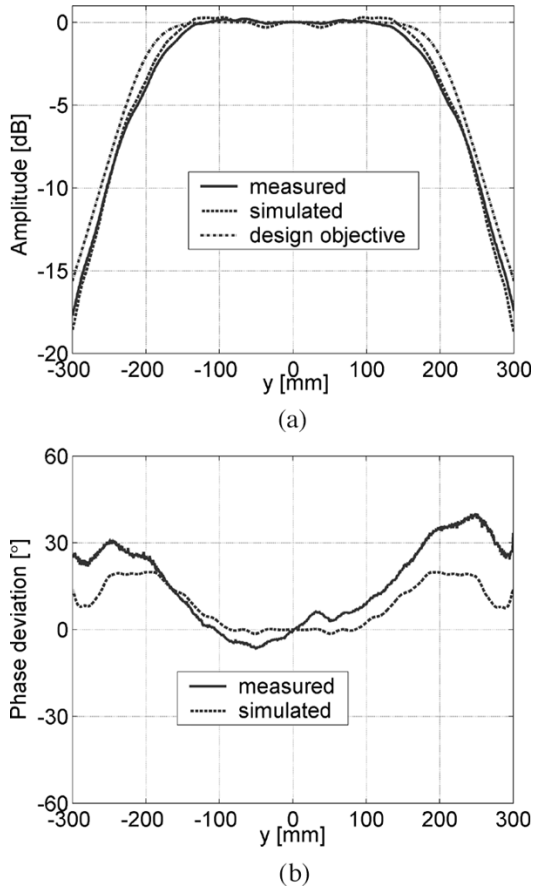

Fig. 7. Measured and simulated (a) amplitude and (b) phase deviation from the spherical wave in a vertical beam cross-cut at 310 GHz.

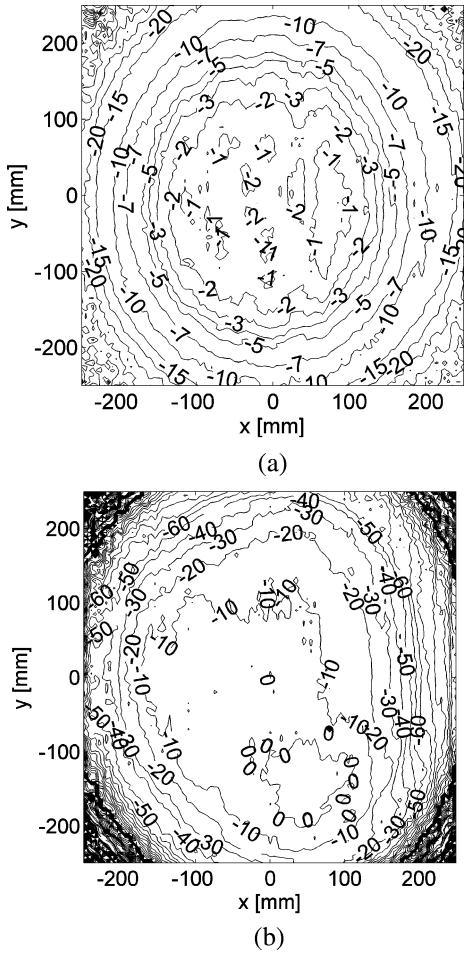

Fig. 8. Measured quiet-zone of the hologram fed by the DRFS: (a) amplitude [dB] and (b) phase [°] at 310 GHz.

to measure the relative distance of outer walls of the DRFS from the scanner probe mounting. The planarity of the probe movement was measured prior the beam measurements using a 3-D tracking laser interferometer and the measured deviations from the planar movement were computationally corrected. Averaging of 10 consecutive scans was used to reduce random probe xy-positioning errors to increase the nominal probe xy-positioning accuracy of 100 μm as within this range the probe position is nearly random. The phase errors caused by the LO cable flexing were corrected using a pilot signal based system [14], which measures the changes in the electrical length of the cable during the measurements. Probe correction was done using the theoretical radiation pattern of the probe and by assuming the DRFS to radiate a spherical wave originating from the hologram focus. After applying these error compensation techniques, the phase measurement uncertainty in a one-dimensional cut of the beam was improved by a factor of two to about $\pm 7^{\circ}$ [14]. Uncertainty in the measured amplitude can be estimated to be a fraction of a dB in the central region of the scan area. The measured and simulated horizontal and vertical cross-cuts of the DRFS beam at 310 GHz are shown in Figs. 6 and 7.

The measured beam corresponds very well to the simulated beam and to the desired hologram illumination. The measured amplitude is within ± 0.3 dB from the simulated amplitude and within ± 0.5 dB from the desired hologram illumination within the radius of 150 mm from the center of the beam. In the same region, which has the most effect on the hologram quiet-zone field, the measured phase is within 30° from the ideal spherical phase. The phase pattern of the feed horn was not compensated in the DRFS synthesis, which is probably the main cause for this slight deviation. However, the measured phase deviations correspond to a change in the focal length of the system in the central region of the beam and this can be compensated by moving the DRFS slightly closer to the hologram so further optimization of the design was not needed. Diffraction effects were not taken into account in the geometrical optics based reflector synthesis. The design could be optimized further to compensate these effects if a higher beam quality is desired.

IV. Measured Quiet-Zone Fields of the Demonstration CATRs

To demonstrate the applicability of the DRFS to hologram based CATRs, a 600 mm diameter hologram was designed for the frequency of 310 GHz. Another hologram with the same size was also designed for direct illumination with a corrugated horn. The quiet-zone amplitude and phase were measured using the same planar scanner and vector network analyzer that were used in the DRFS beam measurements. The quiet-zones of the test holograms were probed with a corrugated horn antenna at a

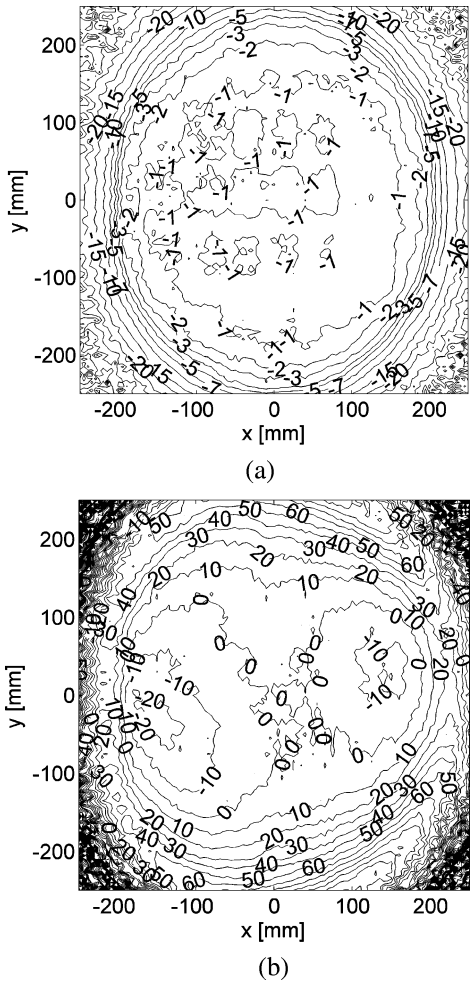

Fig. 9. Measured quiet-zone of the hologram fed by the feed horn directly: (a) amplitude [dB] and (b) phase [°] at 310 GHz.

distance of 1800 mm from the holograms. The same phase measurement error compensation techniques as in the DRFS beam measurements were utilized. As a planar scanner is better suited for measuring a plane wave than a spherical wave, slightly lower uncertainty of $\pm 5^{\circ}$ was achieved in the hologram quiet-zone phase measurements as the probe xy-position errors were considered negligible [14]. The measured contour maps of the amplitude and phase in the quiet-zone of the hologram illuminated by the DRFS are presented in Fig. 8. In Fig. 9, the quiet-zone amplitude and phase at 310 GHz for the hologram illuminated directly by the feed horn, are shown. The amplitudes have been normalized in relation to the maximum value and the phase has been normalized to zero at the center of the measurement area. The 600 mm $\times$ 600 mm area was scanned with 121 consecutive vertical scans. Amplitude and phase drift were compensated by comparing the data in each vertical scan at $y = 0$ to separately measured amplitude and phase at the same points in a horizontal scan and determining the drift correction for each scan. The drift during a single one-dimensional scan taking less than a minute was assumed negligible. The phase measurement uncertainty in a two-dimensional scan is roughly double the uncertainty of a single beam cut, i.e., approximately $\pm 10^{\circ}$ at the corners of the scanned area, and less in the central region, where the quiet-zone is located.

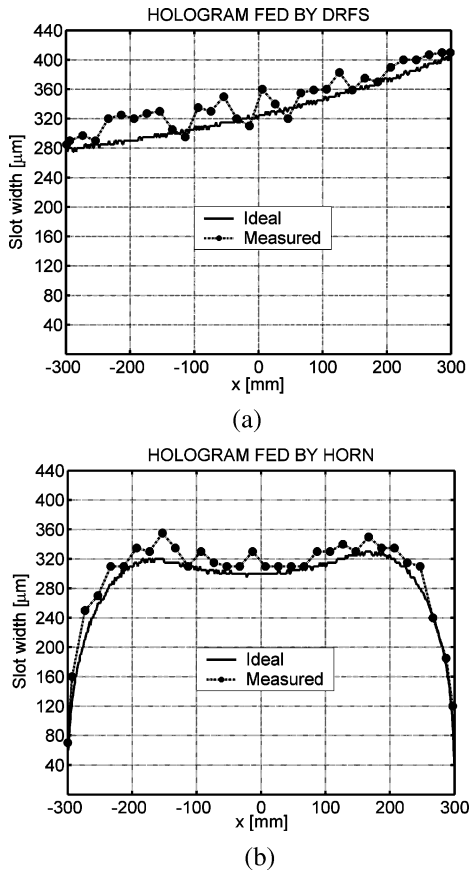

Fig. 10. Slot widths (a) in the hologram with modified illumination and (b) in the hologram with direct illumination with the feed horn.

The root mean squared (rms) amplitude ripple inside a 250 mm diameter circle in the quiet-zone of the hologram illuminated with the DRFS is ± 0.37 dB. The rms phase ripple is $\pm 4.6^{\circ}$. The rms amplitude and phase ripples in the quiet-zone of the hologram fed by the horn directly are ± 0.23 dB and $\pm 4.8^{\circ}$. The quality of the both quiet-zones is in practice identical considering the expected hologram pattern etching accuracy of the order of ± 20 μm with a printed circuit board photolithography process. The diameters of the quiet-zones are approximately 250–300 mm for both holograms. The phase deviations limit the quiet-zone size for the hologram fed by the horn directly and the conservatively selected DRFS beam width limits the quiet-zone size for the DRFS hologram. In principle, the quiet-zone can be enlarged by designing a DRFS with a wider beam with the same edge taper to illuminate the holograms.

V. Improvements to Hologram Based CATRs by Using a Dual Reflector Feed System

A. Hologram Manufacturing

The quality of the quiet-zone field affects the measured radiation pattern of the AUT. The measurement environment and the nonideal operation of the collimating element are the main causes of the ripple and other deviations in the quiet-zone field.

The modified hologram illumination simplifies the hologram manufacturing by eliminating the narrow slots at the hologram pattern edges as narrow slots are difficult to etch accurately,

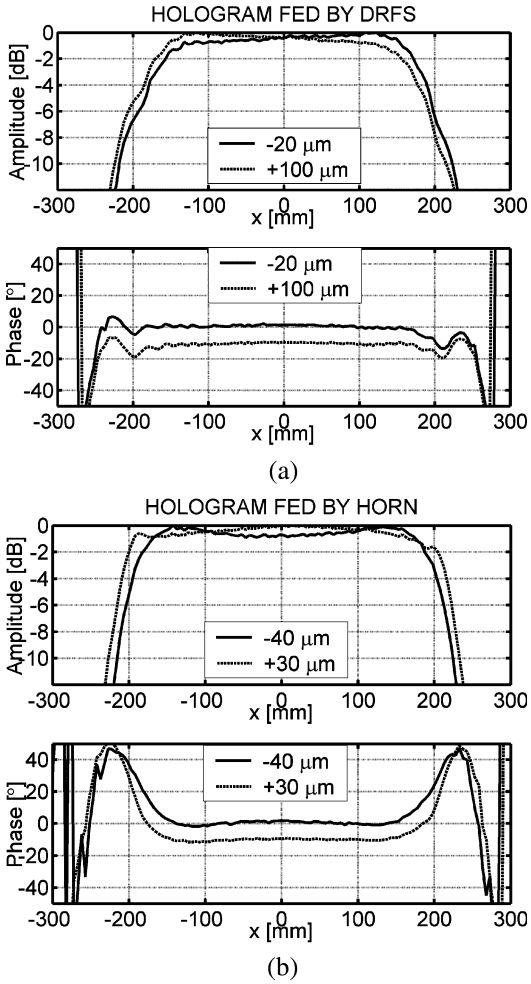

Fig. 11. Simulated horizontal cut of the quiet-zone field (a) for a hologram fed by the DRFS, and (b) for a hologram fed by a corrugated horn directly when a systematic manufacturing error is added to the slot widths of the hologram pattern.

especially in large patterns. The slot width is directly proportional to the wavelength and the elimination of the narrow slots in the hologram pattern is especially significant at shorter submillimeter wavelengths. The slots widths in the hologram illuminated by the DRFS and in the hologram fed with the feed horn directly are shown in Fig. 10. The slot widths were measured with a microscope along the horizontal centerlines of the holograms.

The rms slot width error due to manufacturing errors is about 20 μm for both holograms. This is of the order of the thickness of the metallization (17 μm) of the hologram material (50 μm polyester film, Mylar).

An additional advantage of the modified hologram illumination by the DRFS is that the wider slots are not only easier to etch, but they are also less sensitive to over-etching, i.e., to systematically wider slots, as the relative error in the slot width is smaller for a wider slot when a certain amount of over-etching is present. This can be seen in Fig. 11, where the simulated effect of a systematic error in the slot widths of the hologram pattern on the quiet-zone field is shown. The hologram illuminated with the DRFS can tolerate over-etching of the slots up to 100 μm without significant degradation of the quiet-zone amplitude, as the hologram illuminated directly with the feed horn can tolerate only 30 μm of over-etching. This a significant advantage as over-etching is a common manufacturing error in photolithography processes.

B. Polarization Performance and Quiet-Zone Size

When the hologram is illuminated directly with a feed horn, the amplitude taper has to be realized by tapering the slots in the hologram pattern. However, the transmission of the hologram depends on the polarization. The transmission of a narrow slot is nearly independent of the slot width when the incident field is polarized perpendicular to the slots. Therefore, amplitude taper is difficult to achieve at the horizontal polarization as the slots in the hologram pattern are vertical. By using amplitude taper in the hologram illumination with the DRFS, it should be possible to design holograms that operate at the horizontal polarization. As can be seen in Fig. 9, the hologram quiet-zone is limited by the narrow DRFS beam illuminating the hologram. The quiet-zone size can probably be increased by using a wider shaped beam to illuminate the hologram. This, and the hologram operation at the horizontal polarization, will be investigated in the future.

VI. Conclusion

Modified hologram illumination with amplitude taper can be used to simplify hologram manufacturing for submillimeter wave CATRs. The hologram illumination is shaped with a DRFS. A ray-tracing based shaped reflector synthesis procedure was developed and it was used to design a demonstration DRFS for a hologram based CATR for the frequency of 310 GHz. The DRFS consists of a concave-shaped hyperbolic subreflector and of a convex-shaped hyperbolic main reflector. The system was assembled as an integrated quasioptical system. Performance of the feed system was evaluated with GRASP8W simulations using PO and PTD to compute the radiated beam at 310 GHz. Simulated beam corresponds well to the desired hologram illumination.

The DRFS beam was measured using a planar scanner to probe the field at the location of the hologram at the distance of 1800 mm from the DRFS focus. The measured amplitude and phase show excellent agreement with the simulations; the measured amplitude is within ± 0.3 dB from the simulated amplitude in the beam cross-cuts in the central region of the beam. The measured and simulated phase are within 30° from the desired spherical wave. The slight phase deviation can be compensated by adjusting the DRFS distance from the hologram.

Dual reflector feed system was used to illuminate a test hologram at 310 GHz. The quiet-zone field amplitude and phase were measured and the results were compared to the quiet-zone field of a comparison hologram that was fed directly with a corrugated horn. Both holograms had a diameter of 600 mm. The measured quiet-zones had approximately similar sized quiet-zones, 250–300 mm in diameter, and a similar field quality. The rms amplitude ripples inside a 250 mm diameter circle were ± 0.37 dB and ± 0.23 dB for the DRFS and the reference hologram, respectively. The measured rms phase ripples of the holograms were $\pm 4.6°$ and $\pm 4.8°$, respectively.

The use of the DRFS to illuminate the holograms allows a nearly constant slot width in the hologram pattern, which simplifies the hologram manufacturing by eliminating the narrow slots in the edge of the hologram pattern. Wider slots are easier to etch correctly and they are more tolerant to over-etching. Potential future improvements to the demonstrated system include a wider DRFS beam that would allow a larger quiet-zone for hologram with modified illumination, and, the possibility to design holograms for the horizontal polarization.

ACKNOWLEDGMENT

The authors thank Mr. E. Kahra and Mr. H. Rönnberg for their valuable assistance with the various mechanical constructions and instrumentation. VTT Information Technology is acknowledged for the use of GRASP8W software. Dr. J. Säily is thanked for his development work on the submm wave measurement instrumentation. Dr. J. Mallat and Ms. A. Lönnqvist, and other members of the submillimeter wave research group at Helsinki University of Technology are thanked for their assistance and support. Prof. J. Tuovinen from VTT Information Technology and Mr. J. Lemanczyk from ESA/ESTEC are acknowledged for their advice and support in the hologram CATR development.

REFERENCES

[1] A. Lönnqvist, T. Koskinen, J. Häkli, J. Säily, J. Ala-Laurinaho, J. Mallat, V. Viikari, J. Tuovinen, and A. V. Räisänen, "Hologram-based compact range for submillimeter wave antenna testing," *IEEE Trans. Antennas Propag.*, vol. 53, no. 10, pp. 3151–3159, Oct. 2005.

[2] T. Hirvonen, J. Ala-Laurinaho, J. Tuovinen, and A. V. Räisänen, "A compact antenna test range based on a hologram," *IEEE Trans. Antennas Propag.*, vol. 45, no. 8, pp. 1270–1276, Aug. 1997.

[3] J. Häkli, T. Koskinen, A. Lönnqvist, J. Ala-Laurinaho, J. Säily, J. Mallat, J. Tuovinen, A. V. Räisänen, and J. Lemanczyk, "Dual reflector feed system for submm wave region hologram CATR," in *Proc. 3rd ESA Workshop on Millimeter Wave Technology and Applications*, Espoo, Finland, May 21–23, 2003, pp. 353–358.

[4] J. Häkli, T. Koskinen, J. Ala-Laurinaho, J. Säily, A. Lönnqvist, J. Mallat, J. Tuovinen, and A. V. Räisänen, "A dual reflector feed system for a submm hologram CATR," in *Proc. 13th Int. Symp. Space Terahertz Technology*. Cambridge, MA, 2002, pp. 327–336.

[5] J. Häkli, J. Ala-Laurinaho, and A. V. Räisänen, "Dual reflector feed system for a CATR based on a hologram," in *Proc. Antenna Measurement Techniques Association 25th Annual Meeting and Symp.*, Irvine, CA, 2003, pp. 269–274.

[6] ——, "A numerical synthesis method for designing a shaped dual reflector feed system," *Proc. Inst. Elect. Eng. Microwaves, Antennas and Propagation*, vol. 152, no. 5, pp. 311–318, 2005, to be published.

[7] J. Häkli, J. Ala-Laurinaho, T. Koskinen, J. Säily, A. Lönnqvist, J. Mallat, J. Tuovinen, and A. V. Räisänen, "Synthesis of a dual reflector feed system for a hologram CATR," in *IEEE Antennas and Propagation Society Int. Symp. Dig.*, vol. 4, 2002, pp. 580–583.

[8] P.-S. Kildal, "Synthesis of multireflector antennas by kinematic and dynamic ray tracing," *IEEE Trans. Antennas Propag.*, vol. 38, no. 10, pp. 1587–1599, 1990.

[9] C. S. Lee, "A simple method of dual-reflector geometrical optics synthesis," *Microw. Opt. Technol. Lett.*, vol. 1, no. 10, pp. 367–371, 1988.

[10] J. R. Descardeci and C. G. Parini, "Trireflector compact antenna test range," *Proc. Inst. Elect. Eng. Microwaves, Antennas and Propagation*, vol. 144, no. 5, pp. 119–124, 1997.

[11] J. O. Rubiños-López and A. García-Pino, "A ray-by-ray algorithm for shaping dual-offset reflector antennas," *Microw. Opt. Technol. Lett.*, vol. 15, no. 1, pp. 20–26, 1997.

[12] B. S. Westcott, F. A. Stevens, and F. Brickell, "GO synthesis of offset dual reflectors," *Proc. Inst. Elect. Eng.*, pt. H, vol. 128, no. 1, pp. 11–18, 1981.

[13] A. C. Newell, "Error analysis techniques for planar near-field measurements," *IEEE Trans. Antennas Propag.*, vol. 36, no. 6, pp. 754–768, Jun. 1988.

[14] J. Häkli, J. Säily, J. Ala-Laurinaho, A. Lönnqvist, T. Koskinen, J. Mallat, and A. V. Räisänen, "Improving the measurement accuracy of a planar near-field scanner for submillimeter wave antenna testing," in *Proc. 3rd ESA Workshop on Millimeter Wave Technology*, Espoo, Finland, May 21–23, 2003, pp. 399–405.

[15] J. Säily, P. Eskelinen, and A. V. Räisänen, "Pilot signal based real-time measurement and correction of phase errors caused by microwave cable flexing in planar near-field tests," *IEEE Trans. Antennas Propag.*, vol. 51, no. 2, pp. 195–200, Feb. 2003.

Janne Häkli (S'97–M'05) was born in Helsinki, Finland, in 1972. He received the Master of Science (Tech.) and Licentiate of Science (Tech.) degrees in electrical engineering from the Helsinki University of Technology (TKK), Espoo, Finland, in 1999 and 2002, respectively, and is currently working toward the Doctor of Science (Tech.) degree at TKK.

Since 1998, he has been a Research Assistant and Research Engineer with the Radio Laboratory, TKK. His current research interests include submillimeter-wave shaped reflector antennas, antenna measurement techniques, and hologram applications.

Tomi Koskinen (S'03) was born in Jämsä, Finland, in 1975. He received the Master of Science (Tech.) and Licentiate of Science (Tech.) degrees in electrical engineering from the Helsinki University of Technology (TKK), Espoo, Finland, in 2001 and 2004, respectively, and is currently working toward the Doctor of Science (Tech.) degree at TKK.

Since 2001, he has been a Research Engineer with the Radio Laboratory, TKK. His fields of interest are radio engineering and electromagnetics, especially computational electromagnetics. He is currently developing a hologram-based CATR for very large submillimeter-wave antennas.

Juha Ala-Laurinaho was born in Parkano, Finland, in 1969. He received the Master of Science (Tech.) degree in mathematics, and Licentiate of Science (Tech.) and Doctor of Science (Tech.) degrees in electrical engineering from the Helsinki University of Technology (TKK), Espoo, Finland, in 1995, 1998, and 2001, respectively.

Since 1995, he has been a Research Assistant and Research Engineer with the Radio Laboratory, TKK. His current research interest is the development of antenna measurement techniques for millimeter and submillimeter waves.

Antti V. Räisänen (S'77–M'81–SM'85–F'94) received the Doctor of Science (Tech.) degree in electrical engineering from the Helsinki University of Technology (TKK), Espoo, Finland, in 1981.

In 1989, he was appointed Professor Chair of Radio Engineering, TKK, after holding the same position as an Acting Professor in 1985 and 1987–1989. He has been a Visiting Scientist and Professor with the Five College Radio Astronomy Observatory (FCRAO) and the University of Massachusetts, Amherst, from 1978 to 1981, Chalmers University of Technology, Göteborg, Sweden, in 1983, the Department of Physics, University of California at Berkeley, from 1984–1985, the Jet Propulsion Laboratory, California Institute of Technology, Pasadena, from 1992 to 1993, and the Paris Observatory and University of Paris 6 from 2001 to 2002. He currently supervises research in millimeter-wave components, antennas, receivers and microwave measurements at the Radio Laboratory, TKK, and the Millimeter Wave Laboratory of Finland (MilliLab—European Space Agency (ESA) External Laboratory). The Smart and Novel Radios Research Unit (SMARAD), TKK (which he leads), obtained in 2001 the national status of Center of Excellence in Research from The Academy of Finland after competition and international review. He has authored and co-authored about 400 scientific or technical papers and six books, most recently *Radio Engineering for Wireless Communication and Sensor Applications* (Norwood, MA: Artech House, 2003). He also coauthored the chapter "Radio-Telescope Receivers" in *Radio Astronomy* by J.D. Kraus (Powell, OH: Cygnus-Quasar Books, 1986, 2nd edition).

Dr. Räisänen was the Chairman of the IEEE MTT/AP Chapter in Finland from 1987 to 1992. He was the Secretary General of the 12th European Microwave Conference in 1982, and served as the Conference Chair for the 22nd European Microwave Conference in 1992, and Chair and Co-Chair for the 2nd ESA Workshop on Millimeter Wave Technology and Applications: antennas, circuits and systems in 1998 and the 3rd ESA Workshop on Millimeter Wave Technology and Applications: circuits, systems, and measurement techniques in 2003, respectively. He is Conference Chairman of the International Joint Conference of the 4th ESA Workshop on Millimeter-Wave Technology and Applications, the 8th Topical Symposium on Millimeter Waves TSMMW2006 and the 7th MINT Millimeter-Wave International Symposium MINT-MIS2006 in 2006. During 1995–97 he served in the Research Council for Natural Sciences and Engineering, the Academy of Finland. In 1997, he was elected the Vice-Rector of HUT for the period of 1997–2000. From 2002 to 2005 he served as an Associate Editor of the IEEE TRANSACTIONS ON MICROWAVE THEORY AND TECHNIQUES.